

pyrometer with a vacuum thermopile detector, the multispectral pyrometer with a photomultiplier tube detector and an InSb detector, and the multiwavelength range thermal radiometer with an InSb detector. The results of its application are sufficiently satisfactory.

References

- ¹Yamada, H. Y., "A High Temperature Blackbody Radiation Source," AD 616758, June 1965, p. 26.
- ²Lalos, G. T. et al., "Design and Construction of a Blackbody and Its Use in the Calibration of a Grating Spectroradiometer," *Review of Scientific Instruments*, Vol. 29, June 1958, pp. 505-509.
- ³Gu, S., Fu, G. and Zhang, Q., "3500K High Frequency Induction Heating Blackbody Sources," AIAA Paper 86-1282, June 1986.
- ⁴Dahm, U., "Ein Schwarzer Strahler für hohe Temperaturen," PTB-Mitteilungen, April 1966, pp. 107-109.
- ⁵Quinn, T. J., "The Calculation of the Emissivity of Cylindrical Cavities Giving near Blackbody Radiation," *Temperature Measurements at the National Physical Laboratory, Collected Papers, 1934-1970*, London, 1973, pp. 213-221.
- ⁶Buckley, H., "On the Radiation from the Inside of a Circular Cylinder—Part III," *Philosophical Magazine*, Vol. 17, No. 7, 1934, pp. 576-581.

Natural Convection of a Variable Property Gas in Asymmetrically Heated Square Cavities

Bakhtier Farouk* and Toru Fuseg†
Drexel University, Philadelphia, Pennsylvania

Introduction

NATURAL convection flows of Boussinesq fluids confined in rectangular and cylindrical enclosures have been extensively investigated, and reviews of the literature are found in Ostrach^{1,2} and Catton.³ Although these analyses yield understanding of flows of technological importance, little research effort has been made in investigating the effects of the fluid property variation on the flow and heat transfer characteristics that may be significant when a large temperature difference is present in problems of interest. In order to study these flows, the original Navier-Stokes and energy equations (without simplification by the Boussinesq approximation) must be solved with specified relationships for the fluid property variation.

The properties of different fluids behave differently with temperature. For gases, the specific heat varies only slightly with temperature, density varies inversely with the first power of the absolute temperature, whereas viscosity and thermal conductivity increase with about the 0.8th power of the absolute temperature. Thus, the Prandtl number does not vary significantly with temperature, but viscosity for Newtonian liquids and thermal conductivity for pseudoplastic liquids vary markedly with temperature. Hence, investigations on variable property effects need to be carried out for specific fluids. The effects of the temperature-dependent fluid properties on boundary-layer natural convection flows are reviewed by Kakac et al.⁴ For flows in enclosures, previous investigations⁵⁻¹⁰ consider air as the medium. Zhong et al.⁸ address the

limits of the validity of the Boussinesq approximation for square cavities with differentially heated side walls. They also suggest using a weighted reference temperature for better correlation of heat transfer results. A volume-weighted mean temperature is proposed in Ref. 10 that analyzes the flows in horizontal isothermal concentric cylinders.

The present paper studies convective flows of a variable property gas (air) in an asymmetrically heated square enclosure. The geometry of the problem is shown schematically in Fig. 1. The cavity has a centrally located heated section on its bottom plate and a cooling element on one side wall. These partial heaters are maintained at constant temperatures with different values, whereas the remaining portions of enclosure walls are insulated. The present investigation assumes an infinitely long enclosure.

Mathematical Formulation

The laminar, steady, two-dimensional natural convection flows studied here are described by the Navier-Stokes and energy equations. The viscous dissipation is neglected because of the small magnitude of the velocity induced by natural convection. The governing equation system is

$$\frac{\partial}{\partial x}(\rho u) + \frac{\partial}{\partial y}(\rho v) = 0 \quad (1)$$

$$\begin{aligned} \frac{\partial}{\partial x}(\rho u u) + \frac{\partial}{\partial y}(\rho v u) = -\frac{\partial p}{\partial x} \\ + \text{Pr} \left\{ \frac{\partial}{\partial x} \left[\mu \left(2 \frac{\partial u}{\partial x} - \frac{2}{3} D \right) \right] \right. \\ \left. + \frac{\partial}{\partial y} \left[\mu \left(\frac{\partial u}{\partial y} + \frac{\partial v}{\partial x} \right) \right] \right\} \end{aligned} \quad (2)$$

$$\begin{aligned} \frac{\partial}{\partial x}(\rho u v) + \frac{\partial}{\partial y}(\rho v v) = -\frac{\partial p}{\partial y} \\ + \text{Pr} \left\{ \frac{\partial}{\partial x} \left[\mu \left(\frac{\partial v}{\partial x} + \frac{\partial u}{\partial y} \right) \right] \right. \\ \left. + \frac{\partial}{\partial y} \left[\mu \left(2 \frac{\partial v}{\partial y} - \frac{2}{3} D \right) \right] \right\} - \frac{\text{GrPr}^2}{\epsilon} \rho g \end{aligned} \quad (3)$$

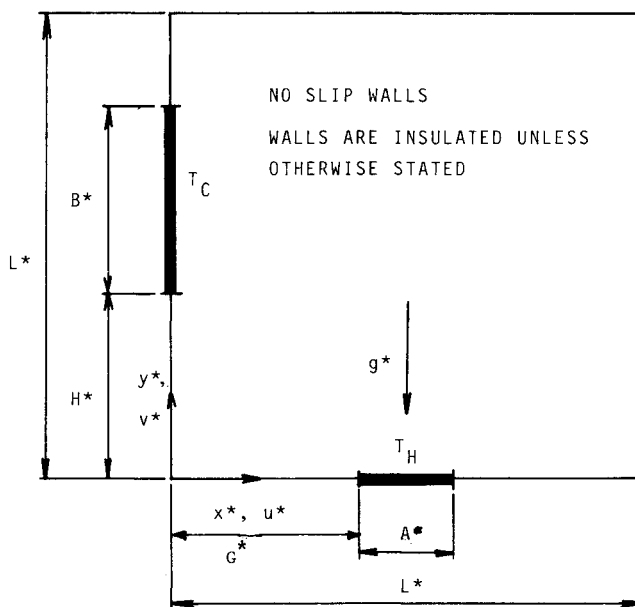


Fig. 1 Geometry and boundary conditions of the problem.

Received Sept. 11, 1986; revision received July 2, 1987. Copyright © American Institute of Aeronautics and Astronautics, Inc., 1987. All rights reserved.

*Associate Professor, Department of Mechanical Engineering.

†Graduate Student, Department of Mechanical Engineering.

$$\begin{aligned} & \frac{\partial}{\partial x} (\rho c_p u T) + \frac{\partial}{\partial y} (\rho c_p v T) \\ &= \frac{\partial}{\partial x} \left(k \frac{\partial T}{\partial x} \right) + \frac{\partial}{\partial y} \left(k \frac{\partial T}{\partial y} \right) \end{aligned} \quad (4)$$

where $D = \partial u / \partial x + \partial v / \partial y$ and ρ , p , μ , g , c_p , and k denote density, pressure, dynamic viscosity, acceleration due to gravity, specific heat, and thermal conductivity, respectively.

The variables are nondimensionalized in the following manner:

$$(x, y) = (x^*, y^*) / A_0, \quad (u, v) = (u^*, v^*) A_0 / \alpha_0$$

$$p = p^* A_0^2 / \rho_0 \alpha_0$$

where α is the thermal diffusivity

$$T = (T^* - T_0) / (T_H - T_C), \quad \phi = \phi^* / \phi_0$$

Variables with an asterisk superscript denote dimensional quantities, and those with a zero subscript denote reference quantities. ϕ stands for ρ , μ , g , c_p , and k .

The Grashof and Prandtl numbers are defined by using the reference quantities as

$$Gr = g_0 \beta_0 \rho_0^2 (T_H - T_C) A_0^3 / \mu_0^2 \quad (5)$$

$$Pr = c_{p0} \mu_0 / k_0 \quad (6)$$

where β is the volumetric thermal expansion coefficient. Parameter ϵ is defined as

$$\epsilon = (T_H - T_C) / T_0 \quad (7)$$

The cold wall temperature was considered here as the reference temperature.

The density variation is computed from the simple ideal gas law whose nondimensional form is expressed as $\rho = p / (\epsilon T + 1)$. For the viscosity and thermal conductivity, the Sutherland formula¹¹ is used: $\phi = s(\epsilon T + 1)^{1.5} / (\epsilon T + s)$ where ϕ stands for μ and k . s is the normalized Sutherland constant that can be expressed for air as $s = 1 + 1.47(T_{bp}/T_0)$, and T_{bp} is the boiling point temperature (78 K for air at 1 atm). The specific heat is assumed constant in the present investigation. From the observation of the foregoing governing equation system, it is seen that the parameter ϵ that represents the magnitude of the buoyancy force also measures the strength of the fluid property variation.

The boundary conditions are stated as follows: $u = v = 0$ at all solid surfaces, $T = 1$ at the heater on the bottom wall ($G \leq x \leq G + A$ with $y = 0$), $T = 0$ at the cooling element on the left side wall ($x = 0$ with $H \leq y \leq H + B$), and $\partial T / \partial n = 0$ everywhere else on the surfaces, where n denotes the coordinate normal to the wall.

Solution Method

The governing equations (1-4) are transformed into a control-volume based, finite-difference equation set. The convection-diffusion terms are discretized by a hybrid scheme.¹² A modified SIMPLE algorithm is used to obtain the steady-state solutions. The present solution procedure differs from the standard method described in Ref. 12. The strongly implicit scheme (SIP) of Stone¹³ is used as the algebraic equation solver instead of the line-by-line scheme based on TDMA. The computations are terminated when the change of all the dependent variables satisfies a specified convergence criterion. The finite-difference mesh system consists of uniformly distributed 42×42 grid points.

Results and Discussion

The computations were carried out for the following parameter ranges: $10^3 \leq Gr.Pr \leq 10^5$ with $Pr = 0.708$ and

$0.2 \leq \epsilon \leq 2.0$. Solutions were also obtained by invoking the Boussinesq approximation, for which the parameter ϵ does not appear explicitly in the formulation. Two different values for the cold element length and position were considered: $B = 2$ with $H = 2$, and $B = 5$ with $H = 0$ (isothermal left side wall) where the length parameters are normalized with the heater length (A_0). The heater length was chosen to be one-fifth of the enclosure length. The temperature of the cold section (T_C) was maintained at 300 K, at which value all the reference fluid properties were evaluated. The highest values of T_H considered is thus 900 K. The reference pressure (p_0) was 1 atm.

Changes in the overall structures of the temperature and flowfields at the reference $Gr.Pr$ of 10^4 are shown in Figs. 2a and 2b. Variable property effects are displayed for ϵ values of 1 and 2. Results obtained by the Boussinesq approximation (for the same Grashof number) are also shown in the same figure. The stream function Ψ was computed from converged velocity fields. The location of the isotherm $T = 0.4$ is seen to be pushed down toward the bottom as the value of ϵ decreases. This indicates that the strength of convection is decreased with increasing values of ϵ due to reduced buoyancy force take off, for a fixed value of the Grashof number. A unicellular flow pattern develops within the enclosure, and as shown in Fig. 2b, the same effect is displayed by the shift of the vortex center (indicted with +) toward the center of the enclosure with increasing values of ϵ . A decrease in the intensity of the flow is also evidenced by the broadening of the distance between the streamlines with

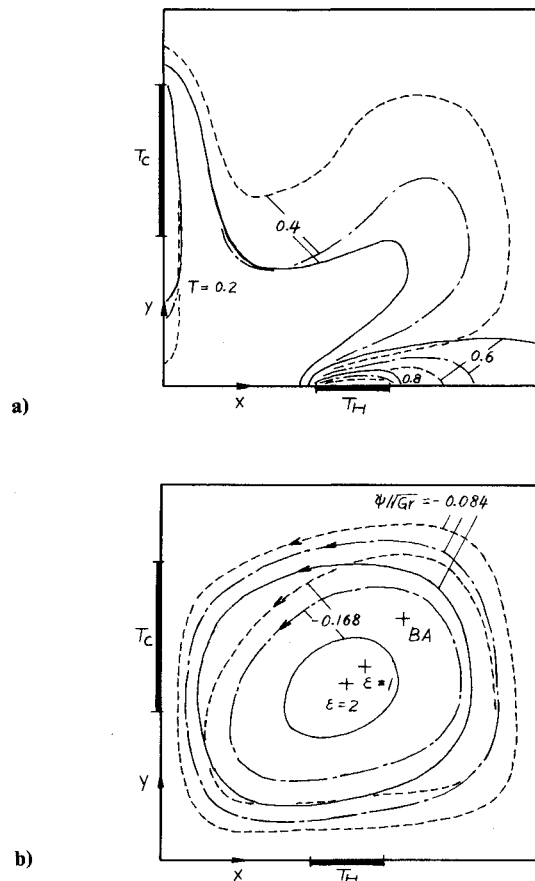


Fig. 2 Comparison of a) isotherms and b) streamlines at $Gr.Pr = 10^4$ for various strengths of the property variation (—, $\epsilon = 2$; - - -, $\epsilon = 1$; ·····, Boussinesq approximation; $B = H = 2$).

Table 1 Maximum absolute values of the stream function and the location where they occur ($B=H=2$)

Gr.Pr	ϵ	$ \Psi _{\max}/\sqrt{Gr}$	(x, y)
10^4	BA ^a	0.241	(3.22, 3.15)
10^4	0.2	0.234	(3.08, 3.04)
10^4	1	0.220	(2.73, 2.53)
10^4	2	0.183	(2.47, 2.27)
10^5	BA	0.148	(3.08, 3.39)
10^5	1	0.125	(2.97, 3.30)
10^5	2	0.114	(2.73, 3.02)

^aBA = Boussinesq approximation.

increasing values of ϵ . When an entirely cold side wall ($B=5$, $H=0$) is considered (results not shown), little change is seen in the field structure except for local deviations in the region near the cold wall, compared to cases with the shorter cooling element ($B=H=2$).

Table 1 shows maximum absolute values of the stream function and their location over the entire range of the parameters investigated (Gr.Pr and ϵ). The intensity of the flow indicated by $|\Psi|_{\max}$ is seen to decrease as ϵ increases for any given Gr.Pr. The shift of the location of the vortex center toward the left lower corner of the cavity accompanies this change. These values also indicate that only a slight increase in the intensity of the flow occurs even when the size of the cooling element is more than doubled.

Conclusions

For the range of the density difference parameter ϵ (≤ 2.0) investigated, the intensity of convection was found to be reduced as ϵ increased. This change appears as the thermal and velocity boundary layers thicken on the enclosure surfaces and the maximum values of the stream function decreases and shift their location toward the cavity center.

References

- ¹Ostrach, S., "Natural Convection in Enclosures," *Advances in Heat Transfer*, Vol. 8, Academic, New York, 1972, pp. 161-227.
- ²Ostrach, S., "Natural Convection Heat Transfer in Cavities and Cells," *Proceedings of the 7th International Heat Transfer Conference*, Vol. 1, 1982, pp. 365-379.
- ³Catton, I., "Natural Convection in Enclosures," *Proceedings at the 6th International Heat Transfer Conference*, Vol. 6, 1978, pp. 13-31.
- ⁴Kakac, S., Atasoglu, O. E., and Yener, Y., "The Effects of the Temperature-Dependent Fluid Properties on Natural Convection—Summary and Review," *Natural Convection, Fundamentals and Applications*, Hemisphere, Washington, DC, 1985, pp. 729-773.
- ⁵MacGregor, R. K. and Emery, A. F., "Free Convection Through Vertical Plane Layers—Moderate and High Prandtl Number Fluids," *Journal of Heat Transfer*, Vol. 91, 1969, pp. 391-403.
- ⁶Rubel, A. and Landis, F., "Laminar Natural Convection in a Rectangular Enclosure with Moderately Large Temperature Differences," *Proceedings of the 4th International Heat Transfer Conference*, Vol. IV, 1970, NC2.10.
- ⁷Leonardi, E. and Reizes, J. A., "Convective Flows in Closed Cavities with Variable Fluid Properties," *Numerical Methods in Heat Transfer*, Vol. 1, Chap. 18, John Wiley, New York, 1981, pp. 387-412.
- ⁸Zhong, Z. Y., Yang, K. T., and Lloyd, J. R., "Variable Property Effects in Laminar Natural Convection in a Square Enclosure," *Journal of Heat Transfer*, Vol. 107, 1985, pp. 133-138.
- ⁹Hessami, M. A., Pollard, A., and Rowe, R. D., "Numerical Calculation of Natural Convective Heat Transfer Between Horizontal Concentric Isothermal Cylinders—Effects of the Variation of the Fluid Properties," *Journal of Heat Transfer*, Vol. 106, 1984, pp. 668-671.
- ¹⁰Mahoney, D. N., Kumer, R., and Bishop, E. H., "Numerical Investigation of Variable Property Effects on Laminar Natural Convection of Gases Between Two Horizontal Isothermal Concentric Cylinders," *Journal of Heat Transfer*, Vol. 108, 1986, pp. 783-788.

¹¹Bretsznajder, S., *Prediction of Transport and Other Physical Properties of Fluids*, Vol. 11, Pergamon Press, Oxford, UK, 1971, pp. 249 and 333.

¹²Patankar, S. V., *Numerical Heat Transfer and Fluid Flow*, Hemisphere, Washington, D.C., 1980, chaps. 5 and 6.

¹³Stone, H. L., "Iterative Solution of Implicit Approximation of Multi-Dimensional Partial Differential Equations," *Journal of Numerical Analysis*, Vol. 5, 1968, pp. 530-558.

Thermocapillary Migration of a Large Gas Slug in a Tube

M. M. Hasan* and R. Balasubramaniam†
NASA Lewis Research Center, Cleveland, Ohio

Nomenclature

- A = temperature gradient at the tube wall
- C_i = constants
- K = nondimensional pressure gradient, Eq. (2)
- L = length of the vapor slug
- Ma = Marangoni number $V_{\infty}R_2/\alpha$
- P, p = pressure, dimensional and nondimensional
- R_1 = radius of the slug
- R_2 = radius of the tube
- t = time
- T = temperature
- V, v = axial velocity, dimensional and nondimensional
- V_{∞} = terminal velocity of the slug
- Z, z = axial coordinate, dimensional and nondimensional
- α = thermal diffusivity
- μ = dynamic viscosity of the liquid
- σ = surface tension
- σ_T = $d\sigma/dT$
- ϕ = dimensionless temperature

Introduction

IN a zero gravity environment, the liquid motion and migration velocities of bubbles and drops in the absence of imposed forced flow will principally be determined by the surface-tension gradient at the interface. The surface-tension gradient may be induced either by a temperature or concentration gradient. The steady thermocapillary motion of bubbles placed in an infinite medium with a linear temperature gradient has been investigated extensively. Young et al.¹ obtained an expression for the terminal velocity of the migration of a bubble, neglecting inertia and the convection of energy. The subsequent studies have relaxed some of the assumptions in Ref. 1. A comprehensive review of the thermocapillary migration of bubbles is given by Thompson.² Balasubramaniam and Chai³ recently reconsidered the problem and obtained an exact solution of the thermocapillary motion of droplets for small Marangoni numbers, but arbitrary Reynolds numbers.

Received Aug. 7, 1987; revision received Jan. 25, 1988. Copyright © 1988 American Institute of Aeronautics and Astronautics, Inc. No copyright is asserted in the United States under Title 17, U.S. Code. The U.S. Government has a royalty-free license to exercise all rights under the copyright claimed herein for Governmental purposes. All other rights are reserved by the copyright owner.

*Aerospace Engineer.

†Resident Research Associate.